^{14}N spin relaxation studies of N_2 in buffer gases. Cross sections for molecular reorientation and rotational energy transfer

Cynthia J. Jameson
Department of Chemistry, University of Illinois at Chicago, Chicago, Illinois 60680
A. Keith Jameson
Department of Chemistry, Loyola University, Chicago, Illinois 60626
Marc A. ter Horst
Department of Chemistry, University of Illinois at Chicago, Chicago, Illinois 60680

(Received 31 December 1990; accepted 12 July 1991)

Nuclear spin–lattice relaxation times (T_1) have been measured as functions of temperature for ^{14}N in N_2 gas and in N_2–Ar, Kr, Xe, CO, CO_2, HCl, CH_4, CF_4, and SF_6 mixtures. The relaxation is dominated by the quadrupolar mechanism so that empirical values of the collision cross sections for molecular reorientation ($\sigma_{\theta,2}$) could be obtained as functions of temperature. The values of $\sigma_{\theta,2}/\text{Å}^2$ at 300 K are 29.6 ± 0.9 (N_2–N_2), 33 ± 1 (N_2–Ar), 41 ± 2 (N_2–Kr), 44 ± 2 (N_2–Xe), 32 ± 1 (N_2–CO), 59 ± 3 (N_2–CO_2), 46 ± 1 (N_2–HCl), 31 ± 1 (N_2–CH_4), 59 ± 2 (N_2–CF_4), and 73 ± 2 (N_2–SF_6). For all $^{14}N_2$–buffer pairs, the temperature dependence of the cross section deviates from T^{-1}, which is not very different from that of the collision cross section (σ_J) for changes in the rotational angular momentum vector. This is the first molecule for which the collision cross sections $\sigma_{\theta,2}$ and σ_J have both been measured for a series of collision partners. The ratio ($\sigma_{\theta,2}/\sigma_J$) is found to be nearly constant, 2.1 ± 0.2 for the N_2 molecule with the ten collision partners. Based on Kouri's IOS factorization scheme, $(\sigma_{\theta,2}/\sigma_J) > 1$ may be true in general. The data for N_2 are compared with the theoretical reduced correlation times based on existing mathematical models for molecular reorientation in fluids.

INTRODUCTION

Nuclear spin relaxation in the gas phase can be used as a measure of the anisotropy of the intermolecular potential.[1] Provided that a single mechanism is responsible for the spin relaxation, a well-defined collision cross section can be obtained from the measurements which may then be used for the refinement of intermolecular potentials. N_2 has been chosen for relaxation studies for several reasons. N_2 is an important component of the atmosphere. The N_2–N_2 dimer is the simplest homonuclear diatomic pair except H_2–H_2. While a fully quantum scattering treatment is needed for H_2–H_2 collisions because the rotational energy levels are so widely spaced, N_2–N_2 collisions may be treated classically or semiclassically. The nuclear quadrupole coupling of the ^{14}N nucleus in N_2 is sufficiently large that the quadrupolar mechanism is the single dominant spin relaxation mechanism in the gas phase, thereby allowing collision cross sections of a specific type ($\sigma_{\theta,2}$) to be extracted from ^{14}N spin–lattice relaxation times (T_1) via the well-established theory of Gordon which relates these two quantities.[1] We have recently completed the determination of another type of collision cross section, that for the relaxation of the angular momentum vector (σ_J), from relaxation times of spin 1/2 ^{15}N nuclei in N_2.[2]

There have been very few measurements of quadrupolar relaxation in the gas phase. Hinshaw and Hubbard studied the quadrupolar ^{11}B relaxation in BF_3 at 270, 300, and 350 K for various densities from about 4 up to about 350 amagat.[3] They found T_1 to be directly proportional to ρ for $\rho \leqslant 22$ amagat and in this range (T_1/ρ) has a temperature dependence of $T^{-0.5 \pm 0.2}$. Gillen *et al.* determined values of the reorientational correlation time, $\tau_{\theta,2}$, from the quadrupolar ^{35}Cl relaxation in ClF in the liquid and gas phases.[4] In the gas phase, at room temperature and for densities between 13 and 22.3 amagat, they report T_1 to vary linearly with density. Their quadrupolar relaxation times were determined directly for the ^{35}Cl nucleus and also indirectly from a combination of rotating frame and spin–lattice relaxation measurements on the ^{19}F nucleus in ClF.

The cross section derived from the quadrupolar relaxation mechanism should provide different information than does the cross section derived from spin–rotation relaxation of the ^{15}N nucleus in the N_2 molecule. The spin–rotation mechanism preferentially weights high J states whereas the quadrupolar mechanism depends primarily on the reorientation of molecules in low J states.[5] Therefore, by studying spin relaxation of the ^{14}N nucleus in the N_2 molecule, complementary information about the intermolecular potential surface can be obtained. Furthermore, tests of model interaction potentials require a multiproperty analysis, which is facilitated by the availability of a wide variety of transport and other cross sections for the N_2 molecule colliding with N_2 and rare gases.[6]

Previous studies have measured spin relaxation times of ^{14}N in the N_2 molecule. Speight and Armstrong report a value of the cross section, $\sigma_{\theta,2}$, and the temperature dependence of (T_1/ρ) based on a study of high density (70–700

J. Chem. Phys. 95 (8), 15 October 1991 0021-9606/91/205799-10$03.00

amagat) nitrogen.[7] These are densities well outside the range in which Gordon's theory, based on binary collisions, applies. Golubev *et al.* measured line widths of nuclear magnetic resonance (NMR) spectra as a function of temperature for $^{15}N_2$ and $^{14}N_2$ in nitrogen gas, from which they determined the spin relaxation times.[8] Their results show substantial relative errors due to the uncertainty in line width measurements. Spin relaxation time measurements in low density gas samples (below 50 amagat) containing $^{14}N_2$ using the inversion recovery method should yield more reliable values for $\sigma_{\theta,2}$ and its temperature dependence. The present work provides the first quadrupolar relaxation studies of the $^{14}N_2$ molecule in various buffer gases. We report temperature dependent cross sections, $\sigma_{\theta,2}$, for N_2 in collisions with N_2, Ar, Kr, Xe, CO, CO_2, HCl, CH_4, CF_4, and SF_6 molecules.

Although a particular cross section for a molecule in a collision pair is uniquely determined by the intermolecular potential function for the collision pair, our previous studies of σ_J for a large number of molecules and collision partners have shown some interesting general trends.[9] It might therefore be expected that a similar global view of $\sigma_{\theta,2}$ could be discerned from systematic studies in the same set of molecules. In particular, it has been noted that $\sigma_{\theta,2}$ is larger than σ_J in the few cases where both have been measured. For example, a combination of ^{19}F rotating frame with ^{19}F spin–lattice relaxation time measurements gives the value $(\sigma_{\theta,2}/\sigma_J) = 1.38$ at room temperature for the ClF molecule in ClF gas.[4] Other methods which provide molecular reorientation cross sections, such as microwave nonresonant absorption (NRA) relaxation, exist only for molecules which have a component of the permanent electric dipole moment along their angular momentum vector.[10] For example, $(\sigma_{\rm NRA}/\sigma_J) = 1.77$ for the NH_3 molecule in gaseous ammonia.[11] Some cross sections for molecular reorientation can be obtained from the viscomagnetic effect $\sigma(02\pi)$, Raman band shapes $(\sigma_{\theta,2})$, and broadening of depolarized Rayleigh line $\sigma(0\hat{2})$. (For definitions of these cross sections see Ref. 12.) These cross sections are related to the $\sigma_{\theta,2}$ from quadrupolar spin relaxation in the classical limit. Just as fluctuations in the orientation of the principal axis of the electric field gradient tensor (which is locked to the molecular framework axis) with respect to the laboratory axes determine the quadrupolar spin relaxation times, the fluctuations in the orientation of the electric polarizability tensor of a molecule determine the collisional line broadening of the depolarized Rayleigh line.[13] For example, $\sigma^{\rm DPR}(0\hat{2})/\sigma_J$ is 1.95 for the CO molecule in carbon monoxide gas,[12,14] and $\sigma^{\rm DPR}(0\hat{2})/\sigma_J = 1.5$ for the CO_2 molecule in carbon dioxide gas,[12,15] and $\sigma^{\rm Raman}_{\theta,2}/\sigma_J$ is 4.2 to 5.1 for CF_4 molecule in CF_4 gas.[16] From these few instances, it appears that $(\sigma_{\theta,2}/\sigma_J) > 1$ might be true in general. However, we need more data before we can conclude this. Thus one motivation for this work is to find the ratio $(\sigma_{\theta,2}/\sigma_J)$ for the N_2 molecule in low density nitrogen gas and for the N_2 molecule in collisions with various partners in mixtures of nitrogen and buffer gases.

A further motivation for this work is in differentiating between existing theories for molecular reorientation. Many models assume that molecular reorientation in a fluid can be characterized by correlation times $\tau_{\theta,n}$, where n is the order of the appropriate Legendre polynomial; the correlation function for the angular momentum vector is similarly characterized by a correlation time τ_J in these models. The details of the dynamics which are assumed in each model lead to different expressions for the correlation times. In the dilute gas in the extreme narrowing limit (i.e., where the collision frequency is greater than the Larmor frequency of the spin), τ_J is a well-defined quantity when one uses the impact approximation and assumes uncorrelated binary collisions. That is, $(1/\tau_J)$ is the rate at which effective collisions randomize both the direction and magnitude of the molecular angular momentum. The average time τ_J between effective collisions is simply the reciprocal of the collision frequency, or in terms of a cross section σ_J

$$\tau_J \equiv (\rho \bar{v} \sigma_J)^{-1}.$$

A similar definition of the effective cross section $\sigma_{\theta,2}$ in $\tau_{\theta,2} \equiv (\rho \bar{v} \sigma_{\theta,2})^{-1}$, comes from the rate $1/\tau_{\theta,2}$ at which effective collisions randomize the direction of the molecule-fixed principal axis of the electric field gradient tensor at a nucleus. In the various models for reorientational motion of molecules in a fluid, the assumptions of the model define one or more of the various correlation times (or the reduced correlation times, defined as $\tau^* \equiv \tau(kT/I)^{1/2}$, where k is Boltzmann's constant, T is the absolute temperature, and I is the vibrationally averaged moment of inertia). Some models, e.g., the Ivanov model, the Hubbard model, the extended diffusion model, the Langevin model, and the friction model, provide both $\tau^*_{\theta,n}$ and τ^*_J. These models predict similar dependences of $\tau^*_{\theta,n}$ on τ^*_J in the liquid phase (i.e., in the limit $\tau^*_J \ll 1$). In the low and intermediate density gas phase (i.e., in the limit $\tau^*_J \gg 1$), these models predict that the ratios should tend toward a constant at low densities but their predictions for the value of this constant vary from 0.75 to 10.05. Therefore gas phase studies have the capacity to test the validity of these models. Earlier attempts to do this have been reported for two molecules. The experimental results for ClF gas[4] lie between the extended diffusion model for linear molecules and the Ivanov model.[17] The CF_4 results[16] follow the *J*-diffusion model for spherical tops.[18] Since we have previously measured σ_J for $^{15}N_2$ molecule in a set of buffer gases,[2] the determination of $\sigma_{\theta,2}$ for $^{14}N_2$ in the same set of buffer gases will provide $\sigma_{\theta,2}/\sigma_J$ which in turn will allow us to find the $\tau^*_J/\tau^*_{\theta,2}$ relationship for these collision pairs in the low to intermediate density regime, for comparison with the predictions of the various models.

EXPERIMENTAL

The gas samples were prepared by condensing a known quantity of the gas in an undersized 4 mm × 5 cm tube maintained at liquid nitrogen temperature. The tube was then sealed from the vacuum line and placed in an oven to be heated above 400 K to ensure the integrity of the sample in the probe at high temperatures. The samples just fit into a 5 mm NMR tube. The densities of the gas samples were between 5 and 40 amagat (1 amagat is the density 2.687×10^{19}

molecule cm^{-3}). The nitrogen densities were corrected for uncondensed gas at liquid nitrogen temperature. We estimate the derived densities to contain less than 4% error. Nitrogen and buffer gases were used as obtained from vendors.

Measurements were made at 28.9 MHz at 9.4 T using a Bruker AM-400 NMR spectrometer. The spin–lattice relaxation times (T_1) were determined from the intensities of the ^{14}N peak obtained using the standard inversion recovery pulse sequence $[\pi - \tau_D - \pi/2 - 5T_1]_n$.[19] Nine different delay times, τ_D, were used. These varied from 0.3 μs, the shortest delay allowed by the spectrometer, up to $5T_1$, the time it takes for the nuclear spins to return to thermal equilibrium. The pulse sequence is repeated n times to obtain the desired signal-to-noise ratio (S/N). Figure 1 shows a typical inversion recovery experiment.

Approximately 6000 transients gave a S/N of at least 40 for all of the samples. The sweep width was set to 20 kHz with an acquisition time of 12.8 ms. For the samples studied, relaxation times ranged from 1.1 to 3.7 ms. The length of the pi pulse ranged from 63 to 85 μs and was determined after tuning the probe at each temperature. The actual temperature was determined from the frequency difference of the proton peaks in an ethylene glycol sample for $T \geqslant 300$ K and in a methanol sample for $T < 300$ K. Dry air was passed over the heater coil for above room temperature experiments and nitrogen gas from liquid nitrogen boil-off for below room temperature work. The accuracy of the temperature is ± 0.5 deg.

Integration of Bloch's equations leads to intensities proportional to bulk magnetization along the applied magnetic field direction which vary with the delay time τ_D as follows:

$$A = A_\infty [1 - \exp(-\tau_D/T_1)] + A_0 \exp(-\tau_D/T_1). \tag{1}$$

The above form accounts for any deviation from the ideal $A_0 = -A_\infty$ owing to B_1 (rf) field inhomogeneity. Even more importantly, for very short relaxation times, Eq. (1) accounts for the finite length of the ideally $\tau_D = 0$ delay. Typical plots of $\ln[(A_\infty - A)/(A_\infty - A_0)]$ vs τ_D are shown in Fig. 2. The slope of these lines is $-1/T_1$. Densities used in this study (5–40 amagat) are all in the extreme narrowing limit, where the spin–lattice relaxation times are proportional to density ρ. In this regime, there is a direct relationship between the measured T_1 and the correlation time $\tau_{\theta,2}$,[1]

$$T_1 = \frac{160 I^2 (2I-1)}{3(2I+3)} \left(\frac{\hbar}{eqQ}\right)^2 \frac{1}{\tau_{\theta,2}}, \tag{2}$$

from which, by $\tau_{\theta,2} = (\rho \bar{v} \sigma_{\theta,2})^{-1}$, we can obtain cross sections directly.

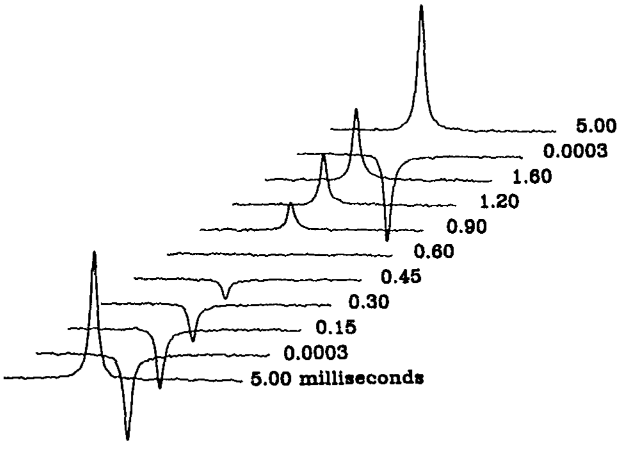

FIG. 1. Typical inversion recovery experiment for ^{14}N in pure N_2 gas (23.6 amagat, 300 K) taken at 28.9 MHz on a Bruker AM-400. Delay times are shown.

Although there are ortho and para species of $^{14}N_2$, a single equation is used here since it has been shown theoretically that the intramolecular quadrupolar relaxation equations for the ortho and para species of X_2 are identical to each other and formally equivalent to those of two uncorrelated nuclear spins; in particular for spin $I = 1$ (such as the ^{14}N nucleus in this work) Bloom *et al.* showed that the relaxation of the magnetization is exponential. The only role played by the identical spins arises from averages of the molecular quantities over the different rotational states of the two species. These differences become vanishingly small at high temperatures, such as those in this study.[20]

A characteristic $(T_1/\rho)_{N_2\text{-}B}$ where B is the buffer gas may be extracted from the T_1 of the mixture using

$$T_1 = (T_1/\rho)_{N_2\text{-}N_2} \rho_{N_2} + (T_1/\rho)_{N_2\text{-}B} \rho_B, \tag{3}$$

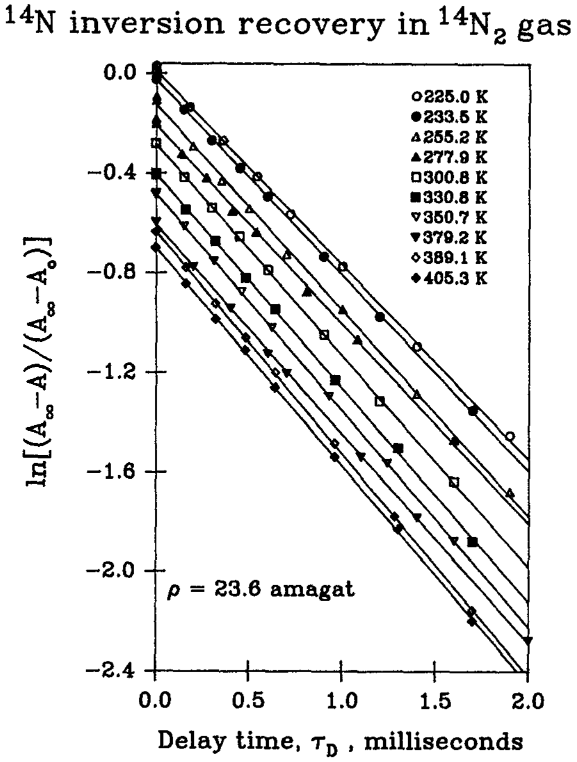

FIG. 2. Typical data for ^{14}N in pure N_2 gas. (The ordinate of each line has been displaced so that all curves may be displayed in the same plot.)

where $(T_1/\rho)_{N_2-N_2}$ is obtained from measurements in the pure gas. The form of Eq. (3) is based on Gordon's theory for spin relaxation in the gas phase in the extreme narrowing limit and has been verified experimentally in our spin–rotation studies of various probe molecules with various buffer gases (see Ref. 2 for references to earlier work).

This form of additivity in the extreme narrowing limit is simply a consequence of the additivity of the collisional contributions of the various molecules in the gas mixture to the collision frequency. Equation (3) can be written for each intramolecular spin relaxation mechanism in this limit. The total relaxation rate would be the sum of the dipolar, the spin–rotation, and the quadrupolar relaxation rates for nitrogen. The natural consequence of this is that, in general, the overall (T_1/ρ) would not depend linearly on mole fraction in binary mixtures. However, we find here that both the dipolar and spin rotation mechanisms are negligibly small in comparison to the quadrupolar. The dipolar and the quadrupolar relaxation mechanisms have the same cross section, so they can be compared directly with each other. From the values of the constants for ^{14}N and the N–N bond length in $^{14}N_2$, we find the ratio of the dipolar to quadrupolar rates is 8.3×10^{-8}; the dipolar contribution can clearly be neglected. Second, in this case we know the spin–rotation relaxation rate independently since we have measured it in the $^{15}N_2$ system.[2] At 300 K the spin–rotation relaxation rate is only 1% of the observed relaxation rate in the $^{14}N_2$ system. For this reason, the spin relaxation in the $^{14}N_2$ system behaves differently from the spin relaxation in the various isotopes of the hydrogen molecule. In the latter the overall (T_1/ρ) does not depend linearly on mole fractions of hydrogen due to the sum of two rates which are comparable in magnitude. On the other hand, the relaxation in $^{14}N_2$ is completely dominated by the quadrupolar mechanism and is found to be well described by Eq. (3). The linear relation given in Eq. (3) occurs when the full matrix multilevel relaxation is replaced by a single effective relaxation time, whereas, it has been shown that a multiple relaxation time treatment is more appropriate.[11] In this study, we find that our experimental data are not sufficiently accurate for a multiple relaxation time treatment. In any case, the latter is unnecessary because nitrogen has so many thermally occupied levels (99% of the molecules are in levels $j=0$ up to $j=19$ at 300 K).

Our analysis differs from that of the very accurately characterized relaxation of hydrogen molecule in mixtures of H_2 in argon.[21] For binary collisions and in the extreme narrowing regime (T_1/ρ) is independent of density. Multiple collision processes in the extreme narrowing regime give rise to an effect which is not present at low densities or high densities and goes through a maximum at a particular density. This was well documented in the H_2–Ar system; the maximum occurs when

$$\rho_{\max}\bar{v}\sigma\approx\omega_{jj},$$

in which σ is the cross section for annihilation of H_2–Ar van der Waals dimers and ω_{jj} is a measure of the magnitude of the anisotropy-induced splittings in the H_2 rotational levels caused by the formation of H_2–Ar dimer. The frequencies ω_{jj} are roughly of the order of magnitude of the rotational constant of the dimer. These splittings have values such that $\rho_{\max}$ occurs at 15 amagat for H_2–Ar. Despite the known existence of van der Waals dimers involving the N_2 molecule, we did not find any reproducible dependence of (T_1/ρ) on the density of the buffer gas in our data. This suggests that $\rho_{\max}$ occurs outside the density range of our experiments. Estimates of the frequencies ω_{jj} for the dimers N_2–X and estimates of annihilation cross sections based on geometric cross sections of the dimers and $\bar{v}$ values at 300 K lead to estimates of $\rho_{\max}$ ranging from 0.2 to 0.7 amagat in various N_2–X mixtures. Thus we do not expect to find a density dependence of (T_1/ρ) in the $^{14}N_2$ relaxation within the range of densities of our samples.

As can be seen in Fig. 3, within experimental error, the temperature dependence of (T_1/ρ) is adequately described by a power law,

$$(T_1/\rho)=(T_1/\rho)_{300\ \mathrm{K}}(T/300)^n. \tag{4}$$

RESULTS

The quantity (T_1/ρ) was found to be independent of density but temperature dependent for each N_2–buffer pair over the density (5–40 amagat) and the temperature ranges studied. Table I shows the temperature dependence of (T_1/ρ) for each N_2–buffer pair and a typical plot is shown in Fig. 3. Every N_2–buffer pair exhibits a temperature de-

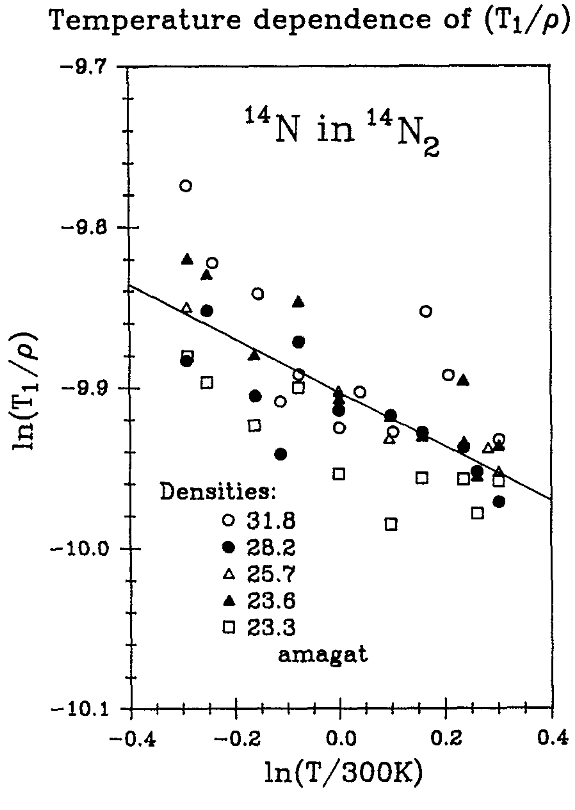

FIG. 3. Typical data showing the temperature dependence of (T_1/ρ) for several samples of pure N_2 gas.

TABLE I. Spin relaxation times for ^{14}N in N_2 with various collision partners.[a] The observed temperature dependence can be described by $(T_1/\rho) = (T_1/\rho)_{300\text{ K}}(T/300)^n$.

Collision partner	$(T_1/\rho)_{300\text{ K}}$ (ms amagat^{-1})	n
CH_4	0.061 ± 0.003	− 0.26 ± 0.06
N_2	0.050 ± 0.002	− 0.17 ± 0.02
CO	0.053 ± 0.002	− 0.19 ± 0.03
Ar	0.052 ± 0.002	− 0.16 ± 0.05
HCl	0.073 ± 0.002	− 0.28 ± 0.06
CO_2	0.089 ± 0.004	− 0.41 ± 0.06
Kr	0.056 ± 0.003	− 0.20 ± 0.06
CF_4	0.081 ± 0.003	− 0.16 ± 0.04
Xe	0.058 ± 0.002	− 0.13 ± 0.05
SF_6	0.095 ± 0.002	− 0.13 ± 0.04

[a] Temperature ranges are: 225–405 K for N_2 in CH_4, N_2, CO, Ar, CO_2, and Kr; 255–405 K for N_2 in Xe; 290–415 K for N_2 in SF_6; 225–415 K for N_2 in CF_4; 280–405 K for N_2 in HCl.

pendence with a negative power. Speight and Armstrong studied ^{14}N spin relaxation in gaseous N_2 at four temperatures ranging from 145 to 380 K and densities ranging from 70 to 700 amagat.[7] To first order, their results give a temperature dependence of (T_1/ρ) which is $T^{0.48 \pm 0.03}$. Typical data for Speight and Armstrong is shown in Fig. 4 (reproduced from their paper)[7] on which is indicated our results at nearly the same temperature. Our data are consistent with theirs, and cover a density range in which the linear dependence of T_1 on ρ is valid. Our temperature dependence of (T_1/ρ) is, however, different from theirs. Their data, on the other hand, provide direct evidence of the theoretically predicted onset of rotational collapse.[22] Golubev *et al.* inferred ^{14}N relaxation times in pure N_2 gas from their measured linewidths at temperatures ranging from 150 to 300 K and densities of about 4 up to 200 amagat.[8] The low precision of their data does not allow the determination of the temperature dependence.

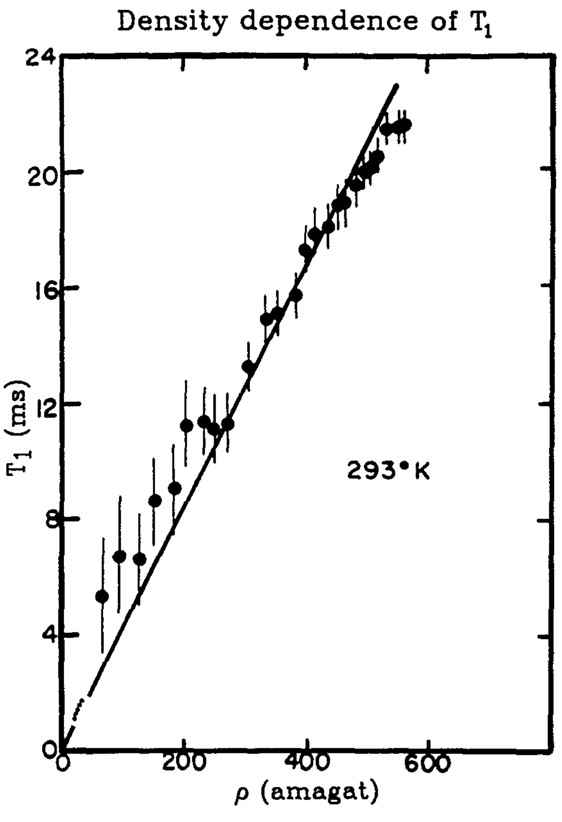

FIG. 4. Comparison of quadrupolar spin relaxation times in low and high density N_2 gas. (The results for high density N_2 reproduced with permission from Ref. 7.) Low density data are at 300 K.

The cross sections for molecular reorientation of N_2 with various buffers at 300 K in Table II were calculated from the measured (T_1/ρ), as indicated in Eq. (2)

$$\left(\frac{T_1}{\rho}\right)_{\text{lin}} = \frac{160 I^2(2I-1)}{3(2I+3)}\left(\frac{\hbar}{eqQ}\right)^2 \bar{v}\sigma_{\theta,2}, \qquad (5)$$

where $\bar{v}$ is the mean relative velocity $(8kT/\pi\mu)^{1/2}$ and eqQ is the nuclear quadrupole coupling constant. The quadrupole coupling constant for N_2 is $eqQ/h = -5.39 \pm 0.05$ MHz determined by Scott from NQR measurements.[23] The cross sections $\sigma_{\theta,2}$ range from 30 to 73 Å^2 for collisions of N_2 with the various molecules which were chosen for their different electronic properties and geometries. The uncertainties listed in Table II are standard deviations and are largely due to uncertainties in densities. There is additional, inconsequential error due to the uncertainty in the magnitude of the quadrupole coupling constant for $^{14}N_2$, not included here. Our value of $\sigma_{\theta,2}$ for $^{14}N_2$ in the pure gas differs from previous reports. The differences are probably due to the fact that the Speight and Armstrong value was taken in higher density samples and the line width measurements conducted by Golubev *et al.* have large uncertainties.

Figure 5 shows the temperature dependence of $\sigma_{\theta,2}$ for N_2 in collisions with various molecules. Consistent with the power law description of $(T_1/\rho)_{\text{lin}}$, we write

$$\sigma_{\theta,2}(T) = \sigma_{\theta,2}(300\text{ K})(T/300)^m. \qquad (6)$$

The powers m and n differ by 1/2 which is the temperature

TABLE II. Quadrupolar relaxation cross sections in N_2 with various collision partners. The observed temperature dependence can be described by $\sigma_{\theta,2}(T) = \sigma_{\theta,2}(300\text{ K})\,(T/300)^m$.

Collision partner	$\sigma_{\theta,2}$(300 K) (Å^2)	m
CH_4	31 ± 1	− 0.76 ± 0.06
N_2	29.6 ± 0.9[a]	− 0.67 ± 0.02
CO	32 ± 1	− 0.69 ± 0.03
Ar	33 ± 1	− 0.66 ± 0.05
HCl	46 ± 1	− 0.78 ± 0.06
CO_2	59 ± 3	− 0.91 ± 0.06
Kr	41 ± 2	− 0.70 ± 0.06
CF_4	59 ± 2	− 0.66 ± 0.04
Xe	44 ± 2	− 0.63 ± 0.05
SF_6	73 ± 2	− 0.63 ± 0.04

[a] This may be compared with 26 Å^2 from Speight and Armstrong (Ref. 7) and 39 Å^2 determined from the data of Golubev *et al.* (Ref. 8) by van Houten *et al.* (Ref. 12).

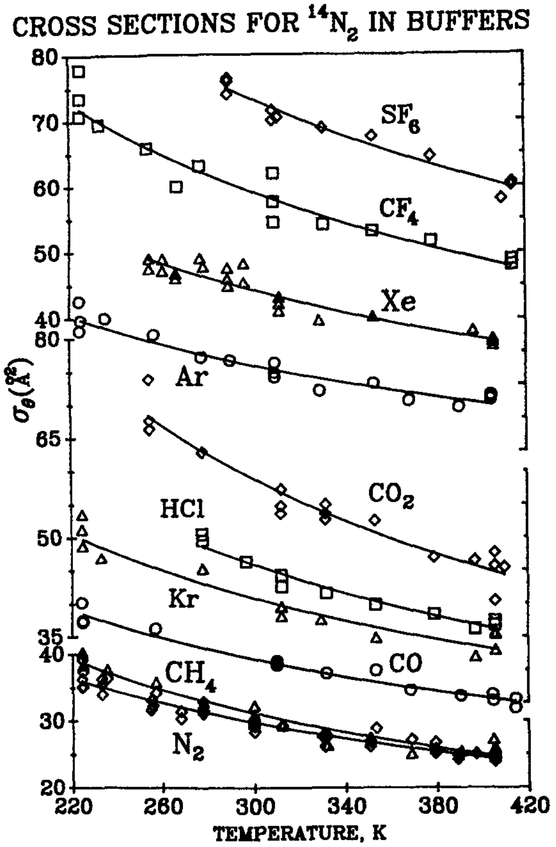

FIG. 5. The temperature dependence of the cross sections $\sigma_\theta(T)$ for N_2 molecule with various collision partners.

dependence implicit in $\bar{v}$. For N_2 in N_2, CH_4, Kr, Ar, and CF_4 gases T_1 data were obtained almost completely from 220 to 410 K and the temperature dependence of the cross sections agrees with Eq. (6). However, for N_2 in HCl, CO_2, Xe, and especially SF_6, the boiling points of the buffers did not permit reliable T_1 data over the complete temperature range. Since the power law description was found adequate for the first set of buffers, Eq. (6) was also applied to the second set of buffers within the limited temperature ranges. The scatter in the $\sigma_{\theta,2}$ vs T plots is due largely to errors in the determination of the densities.

DISCUSSION

The spin–rotation mechanism for spin relaxation depends on those collisions that reorient the molecular angular momentum vector and also those that change the magnitude of the angular momentum. In the thermal average cross section, the high J states are weighted more than a strict population weighting and more than in the quadrupolar mechanism.[5] The quadrupolar mechanism for spin relaxation depends primarily on the reorientational behavior of the observed molecule in its low J states. The contributions to the cross sections from the high J states and low J states involve sampling over different parts of the intermolecular potential. Thus both σ_J and $\sigma_{\theta,2}$ contain information of the anisotropy of the intermolecular potential, but somewhat different information.

From our previous spin–rotation-dominated spin relaxation measurements we have determined the related cross section σ_J for $^{15}N_2$ collisions with the same set of buffer gases. These values at 300 K and the ratios of $\sigma_{\theta,2}$ to σ_J are listed in Table III. The values of $(\sigma_{\theta,2}/\sigma_J)$ range from 1.9 to 2.3 and is 2.1 within experimental error for N_2 in all collision pairs. This is consistent with the ratios found for other molecules in which $(\sigma_{\theta,2}/\sigma_J)$ is greater than unity. For example, $(\sigma_{\theta,2}/\sigma_J)$ for ClF in the pure gas is 1.38.[4] Preliminary results which we now have for $^{14}N^{14}NO$ in various gas mixtures indicate that $(\sigma_{\theta,2}/\sigma_J)$ is 1.1 to 1.4.[24] For spherical tops, on the other hand, the CF_4 data in pure CF_4 gas[16] give ratios of 4.2 to 5.1, very close to 4, while for CH_4 (CD_4) the $(\sigma_{\theta,2}/\sigma_J)$ ratio is 2.94. This is based on $\sigma_{\theta,2}$ for CD_4 molecule obtained from the deuteron relaxation data of Ref. 25 in pure CD_4 gas, and our σ_J for pure CH_4 gas.[26] Additional data on other molecules would be very useful.

From the examples that we have found so far (N_2, ClF, NNO, CH_4, CF_4), it appears that $(\sigma_{\theta,2}/\sigma_J) > 1$ in every case. Is there a fundamental reason why this should be so? To answer this question we have to look at the definitions of $\sigma_{\theta,2}$ and σ_J in terms of Gordon's theory.[5] In the extreme narrowing limit [Eq. (5)]

$$\left(\frac{T_{1Q}}{\rho}\right)_{\text{lin}} = \frac{160 I^2(2I-1)}{3(2I+3)}\left(\frac{\hbar}{eqQ}\right)^2 \bar{v}\sigma_{\theta,2},$$

where the thermal average cross section is

$$\sigma_{\theta,2} = [\mathbf{d}_2 \langle \boldsymbol{\sigma}_2 \rangle^{-1} \mathbf{P} \mathbf{d}_2]^{-1}. \tag{7}$$

Similarly, for a linear molecule

$$\left(\frac{T_{1SR}}{\rho}\right)_{\text{lin}} = \frac{3}{2\langle j(j+1)\rangle C_\perp^2}\bar{v}\sigma_J, \tag{8}$$

where $C_\perp$ is the spin–rotation constant for the observed nucleus in the linear molecule, and

$$\sigma_J = [\mathbf{d}_1 \langle \boldsymbol{\sigma}_1 \rangle^{-1} \mathbf{P} \mathbf{d}_1]^{-1}. \tag{9}$$

Here **P** is the diagonal population matrix, which for a linear molecule is given by

TABLE III. Cross sections determined from relaxation times dominated by the spin–rotation interaction in $^{15}N_2$ with various buffers. $\sigma_J(T) = \sigma_J(300\ \text{K})\ (T/300)^m$.

Collision partner	σ_J (300 K)[a] (Å^2)	m[b]	$\sigma_{\theta,2}/\sigma_J$
CH_4	13.6 ± 0.4	-0.60 ± 0.06	2.3 ± 0.1
N_2	14.9 ± 0.4	-0.70 ± 0.03	1.99 ± 0.08
CO	15.0 ± 0.9	-0.67 ± 0.09	2.1 ± 0.1
Ar	15.9 ± 0.8	-0.74 ± 0.04	2.1 ± 0.1
HCl	22.7 ± 0.6	-0.98 ± 0.02	2.03 ± 0.07
CO_2	29 ± 2	-0.6 ± 0.1	2.0 ± 0.2
Kr	18.1 ± 0.5	-0.74 ± 0.05	2.3 ± 0.1
CF_4	30 ± 1	-0.88 ± 0.04	1.97 ± 0.09
Xe	19.8 ± 0.5	-0.77 ± 0.05	2.2 ± 0.1
SF_6	38.1 ± 0.9	-0.6 ± 0.1	1.92 ± 0.07

[a] Results for $^{15}N_2$–CO_2 and SF_6 are from Ref. 9, all others from Ref. 2.
[b] Results for $^{15}N_2$–CO_2 and SF_6 are unpublished, all others are from Ref. 2.

$$(\mathbf{P})_{j'j} = \delta_{j'j}\,\frac{(2j+1)}{Z_{\mathrm{rot}}}\exp(-E_j/kT), \tag{10}$$

where Z_{rot} is the rotational partition function. For spherical tops there is an additional factor of $(2j+1)$. The vectors $\mathbf{d}_1$ and $\mathbf{d}_2$ are

$$(\mathbf{d}_1)_j = [j(j+1)]^{1/2} \tag{11}$$

$$(\mathbf{d}_2)_j = \left[\frac{j(j+1)}{(2j+3)(2j-1)}\right]^{1/2} \quad \text{for } \Delta j = 0, \tag{12}$$

$$(\mathbf{d}_2)_j = \left[\frac{3(j+2)(j+1)}{2(2j+3)(2j+1)}\right]^{1/2} \quad \text{for } \Delta j = +2, \tag{13}$$

$$(\mathbf{d}_2)_j = \left[\frac{3(j+1)j}{2(2j-1)(2j+1)}\right]^{1/2} \quad \text{for } \Delta j = -2. \tag{14}$$

The sigma matrices $\boldsymbol{\sigma}_1$ and $\boldsymbol{\sigma}_2$, as defined by Neilsen and Gordon, are scattering matrices in line space.[5] Each basis element in this space corresponds to a transition allowed by the selection rule of the rotational angular momentum tensor and the electric field gradient tensor (or electric dipole polarizability tensor), respectively. The sigma matrix represents the effect caused by an average collision of given energy and impact parameter in changing the time development of the tensor. The angular brackets designate thermal averages. The indices in the sigma matrix element $\langle \sigma(j_{\alpha'}j_{\beta'}|j_\alpha j_\beta)\rangle$ represent the states connected by the tensor operator before the collision (α,β) and the states connected after the collision (α',β'). For spin rotation relaxation, $\langle\sigma_1\rangle$ is the scattering matrix for the $\mathbf{J}$ vector, characterized by the selection rule $\Delta j = 0$ so the only nonvanishing sigma matrix elements are $\langle \sigma_1(j'j'|jj)\rangle$. For quadrupolar relaxation the selection rules of the tensor are $\Delta j = 0, \pm 2$. Neilsen and Gordon have shown that only the sigma matrix elements derived from $\Delta j = 0$ need be computed to determine the quadrupolar relaxation at low and moderate densities, i.e., the only elements to consider are $\langle \sigma_2(j'j'|jj)\rangle$. Thus $\langle\sigma_1\rangle$ and $\langle\sigma_2\rangle$ in Eqs. (7) and (9) are matrices with elements

$$\langle\boldsymbol{\sigma}_1\rangle_{j'j} = \langle\sigma_1(j'j'|jj)\rangle,$$

$$\langle\boldsymbol{\sigma}_2\rangle_{j'j} = \langle\sigma_2(j'j'|jj)\rangle.$$

In order to find the relative magnitudes of $\sigma_{\theta,2}$ and σ_J, one could examine corresponding terms in expressions (7) and (9). There are, of course, nonvanishing off-diagonal elements but *if* we assume for the moment that the $\langle\boldsymbol{\sigma}_1\rangle$ and $\langle\boldsymbol{\sigma}_2\rangle$ matrices are diagonally dominant then the matrix elements of the inverse of the matrices are roughly given by

$$(\langle\boldsymbol{\sigma}_1\rangle^{-1})_{j'j} \approx \delta_{j'j}/\langle\sigma_1(jj|jj)\rangle,$$

$$(\langle\boldsymbol{\sigma}_2\rangle^{-1})_{j'j} \approx \delta_{j'j}/\langle\sigma_2(jj|jj)\rangle.$$

With these approximations inserted into Eqs. (7) and (9) we can write the ratio of $\sigma_{\theta,2}$ to σ_J as follows:

$$\frac{\sigma_{\theta,2}}{\sigma_J} \cong \frac{\Sigma_j\, j(j+1)(2j+1)e^{-E_j/kT}/\langle\sigma_1(jj|jj)\rangle}{\Sigma_{j'}\, j'(j'+1)(2j'+1)e^{-E_{j'}/kT}/(2j'+3)(2j'-1)\langle\sigma_2(j'j'|j'j')\rangle}. \tag{15}$$

Kouri[27] has examined the terms in the sums appearing in the numerator and denominator. All the terms in the two sums are positive. The $j = 1$ case was considered separately. If this were the only term in each sum the ratio would range from 4 to 5. This comparison was made possible by using an infinite order sudden (IOS) factorization method which also predicts that the ratio of the thermal averages $\langle\sigma_1(jj|jj)\rangle/\langle\sigma_2(jj|jj)\rangle$ is less than one for all $j > 1$. In addition, the quadrupolar weight $j(j+1)/[(2j+3)(2j-1)]$ is always smaller than the spin–rotation weight $j(j+1)$ for all $j > 0$. These ensure that a term in the numerator is always larger than the corresponding term in the denominator. Thus term by term analysis shows that $(\sigma_{\theta,2}/\sigma_J) > 1$ always. The restrictions on the generality of this conclusion are the applicability of the infinite order sudden approximation to the rotational levels of the linear molecule of interest and the degree of diagonal dominance of the sigma matrices. Comparison with some close coupling calculations showed that $\langle\sigma_1(jj|jj)\rangle < \langle\sigma_2(jj|jj)\rangle$ for $j > 1$ in every case and at all energies reported,[27] which support the general conclusions even though the IOS approximation was used. The same analysis could be applied to a spherical top. Thus we have a satisfactory explanation for our experimental finding that $(\sigma_{\theta,2}/\sigma_J) > 1$. Moreover, based on the above analysis, we expect this to be always the case for linear molecules and spherical tops.

In the preceding analysis we made use of the relative magnitudes of the diagonal elements $\langle\sigma_2(jj|jj)\rangle$ and $\langle\sigma_1(jj|jj)\rangle$ for all j. The full sigma matrices, including off-diagonal elements are determined by the anisotropic parts of the potential and in principle should be different for the N_2 molecule with each different collision partner. We have found in this work a nearly constant ratio of $\sigma_{\theta,2}$ to σ_J regardless of collision partner and nearly independent of temperature, despite the sensitivity of each of $\sigma_{\theta,2}$ and σ_J to the nature of the partner. The near-constancy of the $\sigma_{\theta,2}/\sigma_J$ ratio is a surprising and probably highly significant result of this work. A ratio which is nearly the same for all collision partners seems to indicate that the dependence of $\sigma_{\theta,2}$ and σ_J on the nature of the collision partner is effectively factored out. Is there a fundamental reason why this should be so? We do not have an answer to this yet. First, we need to look at other systems before we can say that this is generally true. The studies on another linear molecule ^{14}N^{14}NO with various collision partners now underway in our laboratory may answer this question in part. We also intend to study the ratio of $\sigma_{\theta,2}$ to σ_J in spherical tops such as CD_4, to see if the ratio is nearly constant for CD_4 irrespective of collision partner.

In a recent paper, we considered our σ_J data for several molecules which are linear or spherical tops, and with a variety of linear and spherical top collision partners.[9] We suggested that the trends in the collision efficiencies for various probe molecules and their collision partners could be very roughly considered to be related to three factors

$$(\sigma_J/\pi d_{12}^2) \propto f\left(\frac{\partial V_{12}}{\partial \theta_1}\right) \cdot g(\alpha_1, \alpha_2, \ldots) \times \left\{\frac{2I_1}{\mu_{12} d_{11}^2} + \frac{1}{2}\left(1 + \frac{I_1 d_{22}^2}{I_2 d_{11}^2}\right)\right\}^{-1}, \qquad (16)$$

where θ_1 is the angle between the probe molecule axis and the line of centers of the collision pair. The factor $f(\partial V_{12}/\partial \theta_1)$ is an electronic factor largely dependent on the anisotropy of the probe molecule as it appears to the approaching (other) molecule. The $g(\alpha_1, \alpha_2, \ldots)$ term is an electronic factor largely dependent on the polarizabilities and the electric moments of the molecules involved in the collisions and was approximated, using Chandler's exponential model,[28] by $\exp(\epsilon_{12}/kT)$, where ϵ_{12} is the average value of the well minimum in the intermolecular potential. The final term is the kinematic factor dependent only on the masses and moments of inertia of the colliding molecules, based on Chandler's model.[29,30] If such an approximate factorization can also be considered for $\sigma_{\theta,2}$, then it is possible that the ratio $(\sigma_{\theta,2}/\sigma_J)$ could be nearly the same, regardless of the collision partner. The collision efficiencies for the N_2 molecule are shown in Table IV.

A number of theoretical models for molecular reorientation in liquids have been proposed in the literature. In some of these models, expressions for some of the reorientational time correlation functions have been derived. Some experiments can provide the correlation functions but more often, only the time integral of these normalized correlation functions, the correlation times, can be obtained. The reorientational correlation times $\tau_{\theta,1}$ and $\tau_{\theta,2}$ describing the time correlation of the first and second order Legendre function and the correlation time for the angular velocity τ_ω (which for linear molecules and spherical tops is also the correlation time for rotational angular momentum, τ_J) are usually converted to the reduced forms, τ^* such that the reduced quantities are in units of the time $(I/kT)^{1/2}$ which is the average time for a classical rotor in thermal equilibrium at a temperature T to rotate by an angle of one radian. In this way, data on different systems can be compared directly. Although the expressions for $\tau_{\theta,1}$, $\tau_{\theta,2}$, and τ_ω are implicit in these models, extracting numerical results from them required further work by Powles and Rickayzen,[31] who have derived continued fraction expressions for the various correlation times and provided tables of numerically computed $\tau_{\theta,1}^*$, $\tau_{\theta,2}^*$, and τ_ω^* (i.e., τ_J^*) values for various models. From these tables we plot $\tau_{\theta,2}^*$ as a function of τ_J^* for linear molecules in Fig. 6. Briefly, these models can be described as follows. The Ivanov model,[32] a rotational random walk generalized by Kluk[33,34] assumes a continuous Markoff process, i.e., the molecule executes a reorientational process uniform in time and on the O_3^+ point group (which transforms the molecular frame into the laboratory frame); the molecule remains stationary between such jumps. The other models are based on versions of the rotational diffusion equation. In the extended diffusion model[18,35] the molecules are assumed to rotate freely during the rotational diffusion step and each step is terminated by a random impulsive torque or collision which randomizes both the orientation and magnitude of the rotational angular momentum vector (J-diffusion limit) or randomizes only the orientation and not the magnitude (M-diffusion limit). The duration of the rotational diffusive steps are random and follow a Poisson distribution. In Fig. 6

TABLE IV. Collision efficiencies for ^{14}N and ^{15}N in N_2 with a set of buffers.

Collision partner	$\sigma_{\rm geom}$[a] (Å^2)	$\sigma_J/\sigma_{\rm geom}$	$\sigma_{\theta,2}/\sigma_{\rm geom}$
CH_4	41.92	0.32	0.74
N_2	41.44	0.36	0.71
CO	40.99	0.37	0.78
Ar	38.05	0.42	0.87
HCl	38.17	0.58	1.21
CO_2	43.13	0.68	1.37
Kr	41.60	0.44	0.99
CF_4	53.59	0.56	1.10
Xe	44.75	0.44	0.98
SF_6	59.28	0.64	1.23

[a] The geometric cross section $\sigma_{\rm geom} = \pi r_0^2$ where r_0 values are taken from G. C. Maitland, M. Rigby, E. B. Smith, and W. A. Wakeham, *Intermolecular Forces, Their Origin and Determination* (Clarendon, Oxford, 1981) (Table A3.2) except for N_2–HCl and N_2–CO which were taken as arithmetic means of r_0 for like pairs, r_0 (CO–CO) = 3.592 Å [R. D. Trengove, J. L. Robjohns, and P. J. Dunlop, Ber. Bunsenges. Phys. Chem. **88**, 450 (1984)] and r_0 (HCl–HCl) = 3.339 Å [A. F. Turfa and R. A. Marcus, J. Chem. Phys. **70**, 3035 (1979)].

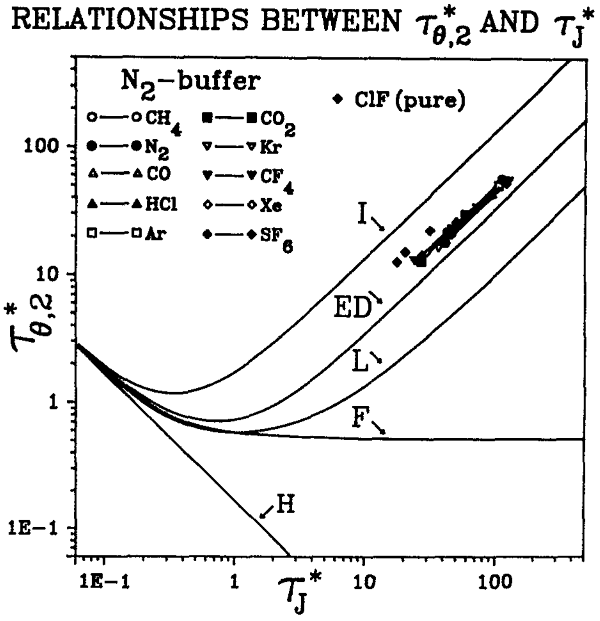

FIG. 6. The dependence of $\tau_{\theta,2}^*$ on τ_J^* predicted by the Ivanov model (I), extended J-diffusion model (ED) for linear molecules, the Langevin model (L), the friction model (F), and the Hubbard model (H) (extended M-diffusion model omitted). Curves are plotted from tables of numbers taken from Ref. 31. Experimental data for N_2 in gas mixtures are from this work and the data for ClF gas were taken from Ref. 4.

we show only the J-diffusion limit for linear molecules. The curve for the M-diffusion limit for linear molecules differs from the J-diffusion limit for $\tau_\omega^* < 1$. The so-called Langevin (L) model[36] is a friction model in which the molecule is taken to be an appropriately shaped object immersed in a continuous viscous fluid. The molecules experience intermolecular torques at all times and each fluctuation in the Brownian torque produces only a slight change in the angular velocity. A large number of fluctuations in the Brownian torque are required for a significant change in the angular velocity. Powles and Rickayzen[31] have obtained explicit results for the Fixman and Rider theory for the correlation times $\tau_{\theta,1}$ and $\tau_{\theta,2}$. The friction (F) model,[37-39] so-called by Powles and Rickayzen, is somewhat misnamed. This model by Steele also assumes that the reorienting molecule is continually subject to intermolecular torques, but instead of the reorientation rate being completely controlled by frictional forces, the molecular motion is characterized by dynamically coherent reorientation over relatively long time intervals in which the correlation function is primarily dependent on inertial parameters (I/kT) rather than friction constants.[37]

The limiting behavior for $\tau_\omega^* < 1$ of these various models (except for the M-diffusion model, not shown in Fig. 6) is

$$\tau_{\theta,2}^* \tau_\omega^* = \tfrac{1}{6}, \quad \tau_\omega^* \ll 1, \tag{17}$$

the so-called Debye limit or Hubbard relation.[31,40] In the limit of a dense fluid at low temperatures, Debye's rotational diffusion model describes the molecular reorientation process well.[18] On the other side, in the limit of dilute gas, for $\tau_\omega^* \gg 1$

$$\begin{aligned} \lim_{\tau_\omega^* \to \infty} (\tau_\omega^*/\tau_{\theta,2}^*) &= 3 \quad \text{extended diffusion} \\ &= 3/4 \quad \text{Ivanov model} \\ &= 10.05... \quad \text{Langevin model} \end{aligned} \tag{18}$$

for linear molecules, and, respectively, 4, 4/5, and 24.4... for spherical tops (not shown in Fig. 6). In the friction model, not expected to be valid for $\tau_\omega^* \gg 1$, $\tau_{\theta,2}^*$ approaches a constant value equal to 5.14.[31]

Included in Fig. 6 are experimental values for the correlation times of N_2 from this study and those of $ClF_{(g)}$ determined by Gillen *et al.*[4] for comparison with the models. Our values of correlation times for N_2 molecule in collisions with a set of collision partners are plotted in Fig. 6 using the moments of inertia[41] of $^{15}N_2$ and $^{14}N_2$ in the $(kT/I)^{1/2}$ reduction factors of τ_J^* and $\tau_{\theta,2}^*$, respectively. The data lie on the curves $\tau_{\theta,2}^*/\tau_J^* \approx 2.1 \pm 0.2$ for N_2 and $\tau_{\theta,2}^*/\tau_J^* = 1.38 \pm 0.15$ for ClF. The slightly different temperature dependences of N_2 with various buffer gases show up as deviations from a slope of 1.0 in this plot. The ratio of correlation times for these two linear molecules do not agree with any specific model of those mentioned; the experimental data lie between the extended diffusion and the Ivanov models. All the models for molecular reorientation in liquids predict a temperature-independent, molecule-independent ratio in the gas limit. While the models predict limiting values which correspond to $(\sigma_{\theta,2}/\sigma_J) = 3$ (extended diffusion), 3/4 (Ivanov), or 10.05 (Langevin), our observed ratios are very nearly 2.1 for N_2 with the various collision partners.

McCourt and co-workers[42,43] have undertaken a comprehensive study of the proposed N_2–rare gas potential energy surfaces, using the infinite order sudden approximation for collision calculations of various properties. Many of the surfaces give relatively good agreement with the transport coefficients (diffusion, sheer viscosity, thermal conductivity) over an extensive temperature range but most are unable to predict the cross sections associated with relaxation phenomena (collision broadening of the depolarized Raman and Rayleigh scattering, viscomagnetic effect). The transport properties are primarily sensitive to the form of the isotropic part of the potential surfaces and are insufficiently sensitive to anisotropies for accurate assessment of the latter. Relaxation phenomena represent sensitive probes of the anisotropy of interaction potentials where state-to-state beam scattering data are not available, and the calculations of McCourt *et al.* clearly bear this out for N_2–He, Ne, and Ar.[43] Multiple property analysis should include relaxation cross sections such as the ones we have obtained here for N_2–other to yield a realistic characterization of the anisotropy of the intermolecular potential surface.

CONCLUSIONS

We have measured the quadrupolar spin relaxation of $^{14}N_2$ in collisions with N_2, Ar, Kr, Xe, CO, CO_2, HCl, CH_4, CF_4, and SF_6 molecules, from which we have obtained by well-established theory, well-defined collision cross sections $\sigma_{\theta,2}$ as a function of temperature. These cross sections for molecular reorientation are found to be 2.1 ± 0.2 times as large as the other well-defined cross section σ_J for changes in the rotational angular momentum vector for the corresponding $^{15}N_2$–other pairs. This is the first observation of the quadrupolar cross section and the first instance where the ratio $\sigma_{\theta,2}/\sigma_J$ has been determined for a molecule with a series of collision partners. The near-constancy of the ratio is intriguing, as is its difference from the few other (ClF–ClF, NH_3–NH_3, CH_4–CH_4, CF_4–CF_4) known ratios. It has been possible to explain in quantum mechanical terms why $(\sigma_{\theta,2}/\sigma_J) > 1$ might be expected in general. Both $\sigma_{\theta,2}$ and σ_J appear to be largely dependent on the anisotropy of the potential surface with respect to the direction of approach of the collision partner. This provides an interesting possibility that $\sigma_{\theta,2}$ and σ_J measured for an N_2 molecule in collisions with HCl, for example, will provide a means of obtaining one set of coefficients in the potential function and the $\sigma_{\theta,2}$ and σ_J measured for an HCl molecule in collisions with N_2 will provide another set.

Comparison of our data on the N_2 molecule in other gases with various classical models for molecular reorientation in fluids shows that in the limit of intermediate density gas, the ratio of reduced correlation times $(\tau_\omega^*/\tau_{\theta,2}^*)$ [or, for uncorrelated binary collisions of linear molecules and spherical tops in the gas phase, the ratio $(\sigma_{\theta,2}/\sigma_J)$] is predicted to be a constant independent of molecule and independent of temperature, and equal to 3 (extended diffusion), 3/4 (Ivanov), or 10.05 (Langevin) for linear molecules. Our observations of a nearly constant ratio 2.1 ± 0.2 over a wide range of temperatures, densities, and buffer gases, agree best with the extended diffusion model.

ACKNOWLEDGMENT

This research has been supported by the National Science Foundation (Grant No. CHE-8901426).

[1] R. G. Gordon, J. Chem. Phys. **44**, 228 (1966).

[2] C. J. Jameson, A. K. Jameson, and N. C. Smith, J. Chem. Phys. **86**, 6833 (1987).

[3] W. S. Hinshaw and P. S. Hubbard, J. Chem. Phys. **54**, 428 (1971).

[4] K. T. Gillen, D. C. Douglass, and J. E. Griffiths, J. Chem. Phys. **69**, 461 (1978).

[5] W. B. Neilsen and R. G. Gordon, J. Chem. Phys. **58**, 4131, 4149 (1973).

[6] A. F. Turfa, J. N. L. Connor, B. J. Thijsse, and J. J. M. Beenakker, Physica A **129**, 439 (1985).

[7] P. A. Speight and R. L. Armstrong, Can. J. Phys. **47**, 1475 (1969).

[8] N. S. Golubev, A. I. Burshtein, and S. I. Temkin, Chem. Phys. Lett. **91**, 139 (1982).

[9] C. J. Jameson and A. K. Jameson, J. Chem. Phys. **93**, 3237 (1990).

[10] G. Birnbaum, Phys. Rev. **150**, 101 (1966).

[11] C. Lemaire and R. L. Armstrong, J. Chem. Phys. **81**, 1626 (1984).

[12] H. van Houten, L. J. F. Hermans, and J. J. M. Beenakker, Physica A **131**, 64 (1985).

[13] H. F. P. Knaap and P. Lallemand, Ann. Rev. Phys. Chem. **26**, 59 (1975).

[14] C. J. Jameson, A. K. Jameson, and K. Buchi, J. Chem. Phys. **85**, 697 (1986).

[15] C. J. Jameson, A. K. Jameson, N. C. Smith, and K. Jackowski, J. Chem. Phys. **86**, 2717 (1987).

[16] J. H. Campbell, S. J. Seymour, and J. Jonas, J. Chem. Phys. **59**, 4151 (1973).

[17] E. Kluk, Mol. Phys. **30**, 1723 (1975).

[18] R. E. D. McClung, J. Chem. Phys. **51**, 3842 (1969).

[19] R. L. Vold, J. S. Waugh, M. P. Klein, and D. E. Phelps, J. Chem. Phys. **48**, 3831 (1968).

[20] M. Bloom, P. Beckmann, and B. Sanctuary, Can. J. Phys. **54**, 2209 (1976).

[21] C. Lemaire and R. L. Armstrong, Can. J. Phys. **63**, 179 (1985).

[22] R. L. Armstrong, *NMR Basic Principles and Progress*, edited by P. Diehl, E. Fluck, and R. Kosfeld (Springer, New York, 1976), Vol. 13, pp. 71–95.

[23] T. A. Scott, Phys. Rep. C **27**, 89 (1976); J. R. Brookeman, M. M. McEnnan, and T. A. Scott, Phys. Rev. B **4**, 3661 (1971).

[24] C. J. Jameson, A. K. Jameson, and M. A. ter Horst (to be published).

[25] P. A. Beckmann, M. Bloom, and E. E. Burnell, J. Chem. Phys. **84**, 5898 (1986).

[26] C. J. Jameson, A. K. Jameson, N. C. Smith, J. K. Hwang, and T. Zia, J. Phys. Chem. **95**, 1092 (1991).

[27] D. J. Kouri, J. Chem. Phys. **69**, 4999 (1978).

[28] H. C. Andersen, D. Chandler, and J. D. Weeks, Adv. Chem. Phys. **34**, 105 (1976).

[29] D. Chandler, J. Chem. Phys. **60**, 3508 (1974).

[30] B. J. Berne and J. A. Montgomery, Jr., Mol. Phys. **32**, 363 (1976).

[31] J. G. Powles and G. Rickayzen, Mol. Phys. **33**, 1207 (1977).

[32] E. N. Ivanov, Zh. Eksp. Teor. Fiz. **45**, 1509 (1963).

[33] E. Kluk and A. Chrzeszczyk, Acta Phys. Pol. A **44**, 409 (1973).

[34] E. Kluk, cited in Ref. 31.

[35] R. G. Gordon, J. Chem. Phys. **44**, 1830 (1966).

[36] M. Fixman and K. Rider, J. Chem. Phys. **51**, 2425 (1969).

[37] W. A. Steele, J. Chem. Phys. **38**, 2404, 2411 (1963).

[38] E. Kluk and J. G. Powles, Mol. Phys. **30**, 1109 (1975).

[39] P. S. Hubbard, Phys. Rev. A **9**, 481 (1974).

[40] P. S. Hubbard, Phys. Rev. **131**, 1155 (1963).

[41] K. P. Huber and G. Herzberg, *Molecular Spectra and Molecular Structure IV. Constants of Diatomic Molecules* (Van Nostrand Rheinhold, Toronto, 1979).

[42] G. C. Corey, F. R. W. McCourt, and G. C. Maitland, Mol. Phys. **62**, 875 (1987).

[43] G. C. Corey, F. R. W. McCourt, and S. Chapman, Mol. Phys. **62**, 897 (1987).